

000 001 002 003 004 005 006 007 008 009 010 011 012 013 014 015 016 017 018 019 020 021 022 023 024 025 026 027 028 029 030 031 032 033 034 035 036 037 038 039 040 041 042 043 044 045 046 047 048 049 050 051 052 053 CTBENCH: CRYPTOCURRENCY TIME SERIES GENERATION BENCHMARK

Anonymous authors

Paper under double-blind review

ABSTRACT

Synthetic time series are vital for data augmentation, stress testing, and prototyping in quantitative finance. Yet in cryptocurrency markets, characterized by 24/7 trading, extreme volatility, and rapid regime shifts, existing Time Series Generation (TSG) methods and benchmarks often fall short, jeopardizing practical utility. Most prior work targets non-financial or traditional financial domains, focuses narrowly on classification and forecasting while neglecting crypto-specific complexities, and lacks critical financial evaluations, particularly for trading applications. To bridge these gaps, we introduce **CTBench**, the first Cryptocurrency Time series generation **Benchmark**. It curates an open-source dataset of 452 tokens and evaluates models across 13 metrics spanning forecasting accuracy, rank fidelity, trading performance, risk assessment, and computational efficiency. A key innovation is a dual-task evaluation framework: the Predictive Utility measures how well synthetic data preserves temporal and cross-sectional patterns for forecasting, while the Statistical Arbitrage assesses whether reconstructed series support mean-reverting signals for trading. We systematically benchmark eight state-of-the-art models from five TSG families across four market regimes, revealing trade-offs between statistical quality and real-world profitability. Notably, CTBench provides ranking analysis and practical guidance for deploying TSG models in crypto analytics and trading applications. The source code is available at <https://anonymous.4open.science/r/CTBench-F5A3/>.

1 INTRODUCTION

Time Series Generation (TSG) has become foundational for numerous downstream tasks, including data augmentation (Bao et al., 2024; Ramponi et al., 2018), anomaly detection (Ang et al., 2023b; Wang et al., 2021), privacy preservation (Jordon et al., 2018; Tian et al., 2024), and domain adaptation (Cai et al., 2021; Li et al., 2022b). The core objective of TSG is to synthesize sequences that preserve the temporal dependencies and structural characteristics of real-world data. Despite growing interest, the vast majority of existing TSG benchmarks and methods target domains such as healthcare, mobility, or sensor data (Ang et al., 2023a; 2024). Financial time series, which are inherently noisy, non-stationary, and adversarial, remain underexplored in the context of generative modeling. More importantly, even financial TSG efforts primarily focus on stock data (Yoon et al., 2019; Wiese et al., 2020), often under simplifying assumptions that fail to generalize to emerging financial modalities. Consequently, the unique characteristics of modern financial markets, particularly in the digital asset space, are largely overlooked.

Cryptocurrencies, as a prominent subclass of financial time series with a global market capitalization exceeding \$4 trillion as of May 2025 (Reuters, 2025), introduce new modeling and evaluation challenges. Unlike traditional financial instruments, crypto markets operate 24/7, lack intrinsic valuation anchors, and exhibit extreme volatility driven by speculation, fragmented liquidity, and decentralized exchange infrastructure. These properties violate assumptions embedded in existing financial benchmarks (Hu et al., 2025; Wang et al., 2025; Qiu et al., 2024), which typically rely on regular trading hours, stable macroeconomic signals, or broad stationarity assumptions.

While recent benchmarks for financial time series, such as FinTSB (Hu et al., 2025) and FinTS-Bridge (Wang et al., 2025), have advanced evaluation practices, they fall short in three critical aspects when applied to cryptocurrency settings:

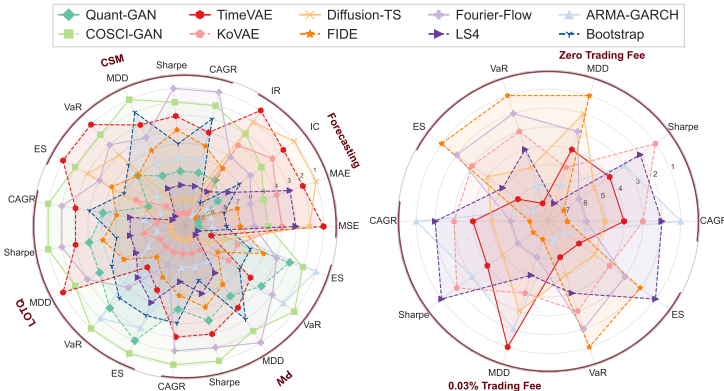


Figure 1: **Aggregate rankings of eight TSG models on both tasks from 2021 to 2024: Predictive Utility (left) assesses fidelity and predictive signal quality, and Statistical Arbitrage (right) evaluates trading performance under realistic fee conditions.** The results reveal distinct trade-offs across fidelity, tradability, and robustness, with no model uniformly dominating all measures.

- **Limited Domain Generality:** Existing works (Ang et al., 2023a; Hu et al., 2025) focus primarily on traditional assets such as equities and indices (e.g., SPX and CSI300) with lower volatility and restricted trading hours, offering minimal support for cryptocurrency data. They overlook the high-frequency, 24/7 dynamics of crypto markets.
- **Narrow Task Scope:** Most financial time series benchmarks emphasize classification and forecasting, neglecting generation and trading-centric tasks like arbitrage, which are vital for crypto-specific applications such as arbitrage and market-neutral strategies. Moreover, TSG methods in crypto contexts remain largely unexplored.
- **Lack of Crypto-Specific Evaluation:** Existing benchmarks underrepresent measures needed to assess real trading utility. While TSGBench focuses on statistical fidelity, and FinTSB introduces limited financial metrics, both rely on assumptions from traditional markets, failing to continuous trading, heavy-tailed risk, and actionable signal quality unique to crypto assets.

To address these limitations, we introduce **CTBench**, the first Cryptocurrency Time series generation **Benchmark**. It is an open-source benchmark for rigorous evaluation of TSG methods in cryptocurrency markets, with three key contributions:

- **Crypto-Centric Dataset.** We provide a curated cryptocurrency dataset from major global exchanges, processed via a standardized pipeline with crypto-specific feature support. This ensures analysis-ready data reflecting the volatility and structural nuances of crypto markets.
- **Dual-Task Benchmarks.** To operationalize the utility of synthetic data in real-world finance, CTBench introduces a dual-task evaluation framework that jointly assesses predictive fidelity and tradability. The Predictive Utility task trains forecasters on synthetic data and tests them on real returns, while the Statistical Arbitrage task evaluates whether reconstructed residuals yield tradable mean-reverting signals.
- **Financial Metric Suite.** CTBench introduces a comprehensive evaluation suite over diverse trading strategies spanning forecasting accuracy, rank-based measures, trading performance, and risk metrics, designed to reflect crypto-specific market realities.

We benchmark eight state-of-the-art TSG models and analyze trade-offs across fidelity, tradability, and robustness. Figure 1 shows aggregate rankings across two tasks, with measures radially arranged and averaged over strategies and fee settings. No model dominates universally, highlighting distinct trade-offs between fidelity, tradability, and robustness, and underscoring CTBench’s value for informed model selection in crypto trading contexts.

2 PRELIMINARIES

Let $\mathbf{R} \in \mathbb{R}^{n \times l}$ denote the log-return matrix, where n is the number of tradable crypto-assets and l is the number of hourly return observations. At each time $t \geq 1$, the log-return vector across all assets is $\mathbf{r}_t = [r_{1,t}, \dots, r_{n,t}] \in \mathbb{R}^n$, where each element is defined as $r_{i,t} = \log \frac{p_{i,t}}{p_{i,t-1}}$, with $p_{i,t}$ the price of asset i at hour t . To mimic real-world backtesting, we employ a rolling-window

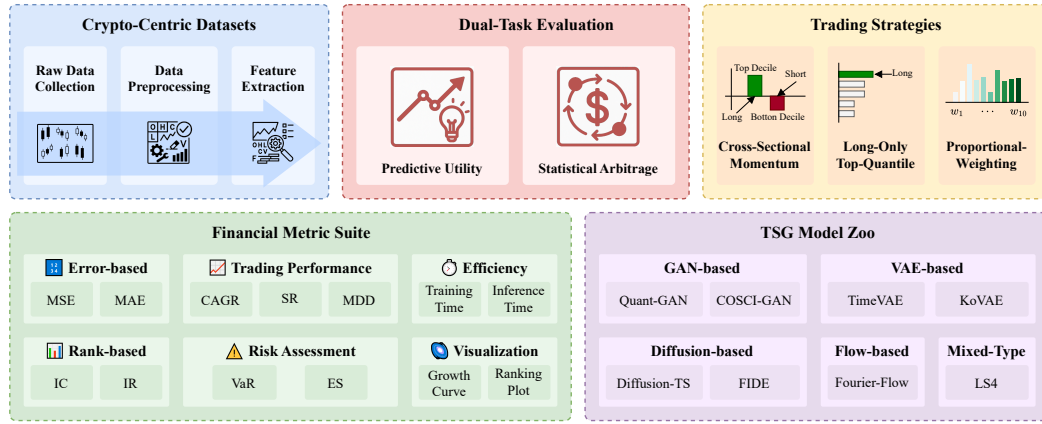


Figure 2: Overall architecture of **CTBench**. The framework unifies five modules: (1) crypto-centric datasets, (2) dual-task evaluation (predictive utility and statistical arbitrage), (3) trading strategies, (4) comprehensive financial metrics, and (5) diverse TSG models into a unified benchmark pipeline.

protocol: Given a training window size w and a test step s , we define split offsets $\tau \in \mathcal{O} = \{w, w+s, \dots, w+(k-1)s\}$, where $k = \lfloor \frac{w}{s} \rfloor$. Each offset τ yields a training and test split:

$$\mathbf{R}_{\text{train}}^{(\tau)} = [\mathbf{r}_{\tau-w+1}, \dots, \mathbf{r}_\tau], \mathbf{R}_{\text{test}}^{(\tau)} = [\mathbf{r}_{\tau+1}, \dots, \mathbf{r}_{\tau+s}].$$

For each split, a TSG model $\mathbf{g}^{(\tau)}$ is trained on $\mathbf{R}_{\text{train}}^{(\tau)}$ and evaluated in two modes: (1) **Generation Mode**: sampling synthetic sequences from Gaussian noise, $\mathbf{R}_{\text{gen}} = \mathbf{g}^{(\tau)}(\mathbf{z})$, $\mathbf{z} \sim \mathcal{N}(\mathbf{0}, \mathbf{I})$; (2) **Reconstruction Mode**: reconstructing training and test set, $\hat{\mathbf{R}}_{\text{train}} = \mathbf{g}^{(\tau)}(\mathbf{R}_{\text{train}}^{(\tau)})$, $\hat{\mathbf{R}}_{\text{test}} = \mathbf{g}^{(\tau)}(\mathbf{R}_{\text{test}}^{(\tau)})$.

We further define a basic portfolio simulation setup: Starting with initial capital $V_0 > 0$, the strategy allocates weights $\boldsymbol{\eta}_t = [\eta_{1,t}, \dots, \eta_{n,t}] \in \mathbb{R}^n$ at each hour t , where $\eta_{i,t}$ denotes the fraction invested in asset i . The portfolio value then evolves as $V_t = V_{t-1} \times (\boldsymbol{\eta}_t \cdot \mathbf{r}_t)$, with hourly profit-and-loss given by $\Delta V_t = V_t - V_{t-1}$. A summary of notations is provided in Appendix A. To maintain clarity and scope, CTBench restricts its benchmark design to datasets, trading strategies, evaluation measures, and TSG models, as detailed in Appendix B.

3 CTBENCH

We present **CTBench**, the first benchmark specifically designed to evaluate Time Series Generation (TSG) models in cryptocurrency markets (Figure 2).

3.1 CRYPTO-CENTRIC DATASETS

Data Overview and Preprocessing. Our benchmark leverages historical hourly data from all USDT-denominated spot pairs on Binance (Binance Exchange, 2025b), spanning January 2020 to December 2024 and capturing diverse market regimes such as bull runs, crashes, and consolidation phases. To ensure quality, we exclude assets with missing records and retain only USDT pairs, yielding 452 unique cryptocurrencies, a robust foundation for TSG evaluation.

Formally, let n denote the number of tradable crypto assets and $(l+1)$ the number of hourly observations. Each asset $i \in \{1, \dots, n\}$ at time $t \in \{0, \dots, l\}$ is represented by four standard fields:

$$\mathbf{x}_{i,t} = [O_{i,t}, H_{i,t}, L_{i,t}, C_{i,t}] \in \mathbb{R}^4,$$

where O , H , L , and C are the **Open**, **High**, **Low**, and **Close** prices (quoted in USDT), respectively. Stacking across all assets yields the multi-asset OHLC data array: $\mathbf{D} = [\mathbf{x}_{i,t}] \in \mathbb{R}^{n \times (l+1) \times 4}$. We focus primarily on **Close** prices and define hourly log-returns as: $r_{i,t} = \log \frac{C_{i,t}}{C_{i,t-1}}$, where $t \in \{1, \dots, l\}$, giving the return matrix $\mathbf{R} \in \mathbb{R}^{n \times l}$.

Feature Extraction. To capture key market dynamics, we extract d features widely used in quantitative trading, such as Alpha101 factors (Kakushadze, 2016), Bollinger Bands, RSI, and moving

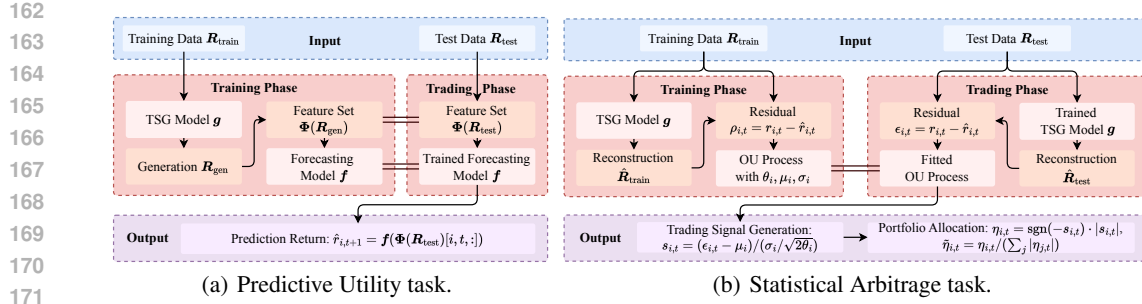


Figure 3: Architectures of dual-task benchmarks.

averages (Sun et al., 2023; Zhu & Zhu, 2025; Zhang et al., 2020; Tsai & Hsiao, 2010). These features encode signals such as momentum, mean-reversion, and volatility. Applying the same pipeline to both real and synthetic data enables consistent evaluation of TSG models’ ability to replicate the statistical and structural properties vital for downstream tasks.

Formally, let $\Phi = \{\phi_j\}_{j=1}^d$ be the feature set, where each $\phi_j : \mathbb{R}^{n \times l} \rightarrow \mathbb{R}^{n \times l}$ acts on the return matrix \mathbf{R} . Applying Φ yields a feature tensor with shape $\mathbb{R}^{n \times l \times d}$. The dataset exhibits strong cross-sectional dispersion and cap-dependent volatility, motivating crypto-specific evaluation of predictive structure and cross-asset dynamics beyond marginal similarity (see Appendix C.1).

3.2 DUAL-TASK EVALUATION

To connect generation fidelity with financial utility, CTBench introduces dual-task evaluation assessing both predictive realism and tradable structure. As shown in Figure 3, these tasks measure whether synthetic data preserves useful forecasting signals (predictive utility) or enables the discovery of stationary, market-neutral alpha (statistical arbitrage). Details are in Appendix C.2.

Predictive Utility Task. This task tests whether synthetic data can train forecasting models that generalize to real markets. As shown in Figure 3(a), given a training log-return window $\mathbf{R}_{\text{train}}^{(\tau)}$, a TSG model g generates synthetic returns $\mathbf{R}_{\text{gen}} = g(z)$, $z \sim \mathcal{N}(\mathbf{0}, \mathbf{I})$. Features $\Phi(\mathbf{R}_{\text{gen}})$ are then extracted and used to train a forecasting model f instantiated as XGBoost (Chen & Guestrin, 2016) for its robustness to heterogeneous features and noisy financial environments (Vancsura et al., 2025; Liu et al., 2021; Yun et al., 2021). The ablation study in §4.4 comparing additional forecasters confirms that XGBoost uniquely balances low prediction error with strong cross-sectional ranking fidelity, a property essential for downstream trading evaluation.

The trained f is deployed on real test data \mathbf{R}_{test} to generate signals for a dollar-neutral long-short portfolio, rebalanced hourly over a month. This setup tests whether \mathbf{R}_{gen} preserves predictive signals with measurable economic value. All components, TSG model, features, and forecaster, are modular, allowing extensibility across architectures.

Statistical Arbitrage Task. In contrast to the generation-focused task, this task evaluates whether TSG models can reconstruct market structure and isolate tradable, mean-reverting residuals for statistical arbitrage. As depicted in Figure 3(b), a model g is trained on real returns $\mathbf{R}_{\text{train}}$ to produce reconstructions $\hat{\mathbf{R}}_{\text{train}}$, and the residuals $\rho_{i,t} = r_{i,t} - \hat{r}_{i,t}$ are assumed to follow Ornstein–Uhlenbeck (OU) processes (Uhlenbeck & Ornstein, 1930), parameterized by estimated $(\mu_i, \theta_i, \sigma_i)$ per asset.

On test data, new residuals $\epsilon_{i,t}$ are mapped to standardized $s_{i,t} = (\epsilon_{i,t} - \mu_i) / (\sigma_i / \sqrt{2\theta_i})$, which drive trading decisions via thresholding ($\gamma = 2$) and weight normalization. Portfolios are rebalanced hourly based on these signals. This task complements generation-focused evaluation by assessing the model’s ability to reveal stationary, market-neutral alpha, thus bridging statistical fidelity and practical trading utility.

3.3 TRADING STRATEGIES

CTBench is strategy-agnostic, allowing TSG models to be evaluated across diverse trading paradigms. Rather than relying on a single approach, we compute profitability and risk metrics (§3.4) consistently for all backtests. This enables rigorous stress testing and reveals whether

216 TSG models capture genuine market structure or merely overfit specific trading styles. We evaluate
 217 models under three canonical trading strategies commonly adopted in cryptocurrency markets:
 218

- 219 • **Cross-Sectional Momentum (CSM):** take long positions in the top decile of predicted assets
 220 while shorting the bottom decile, capturing relative momentum effects.
- 221 • **Long-Only Top-Quantile (LOTQ):** build an equal-weight portfolio of the top 20% of assets,
 222 reflecting long-biased strategies often favored in practice.
- 223 • **Proportional Weighting (PW):** allocate capital in proportion to predicted returns, directly trans-
 224 lating forecasts into position sizes.

225 This modular design supports plug-and-play integration of additional or proprietary strategies. Full
 226 details are provided in Appendix C.3.

227 3.4 FINANCIAL METRIC SUITE

228 Evaluating TSG models for financial applications requires more than mere statistical similarity, it
 229 demands measuring whether synthetic data enables profitable and risk-aware trading. To this end,
 230 CTBench defines thirteen core metrics, grouped into six practitioner-relevant categories:
 231

- 232 • **Error-based Evaluation:** At the most fundamental level, do synthetic returns numerically re-
 233 semble real ones? Metrics include Mean Squared Error (**MSE**), which emphasizes volatility
 234 mismatches, and Mean Absolute Error (**MAE**), which is more robust to outliers.
- 235 • **Rank-based Evaluation:** Do synthetic returns preserve relative asset ordering? Information
 236 Coefficient (**IC**) measures rank correlation, and Information Ratio (**IR**) evaluates its stability.
- 237 • **Trading Performance:** Does synthetic data yield actionable, profitable signals? Statistical accu-
 238 racy does not guarantee financial profitability. We therefore use Compound Annual Growth Rate
 239 (**CAGR**) for long-term growth and Sharpe Ratio (**SR**) for return-to-risk balance.
- 240 • **Risk Assessment Metrics:** Do models capture fat tails and downside risks? We compute Max-
 241 imum Drawdown (**MDD**) for worst-case loss, Value at Risk (**VaR**) at 95% confidence, and Ex-
 242 pected Shortfall (**ES**) for tail risk beyond VaR.
- 243 • **Efficiency:** Can models support real-time deployment? We track **Training Time** and **Inference**
 244 **Time** to assess adaptability in fast-moving crypto markets.
- 245 • **Visualization:** Do results exhibit contextual realism? We report **Simulated Growth Curves**
 246 for a \$10,000 investment and cross-sectional **Ranking Plots** across market regimes to illustrate
 247 interpretability and contextual realism.

248 Together, these metrics ensure balanced evaluation of fidelity, utility, and practicality. Full defini-
 249 tions are in Appendix C.4.

250 3.5 TSG MODEL ZOO

251 Generative models for time series aim to capture temporal dependencies and structural patterns, with
 252 backbones spanning GANs, VAEs, diffusion models, flow models, and mixed-type models (Ang
 253 et al., 2023a; Nikitin et al., 2023) (see Table 3). Yet, nearly half of prior TSG works do not evaluate
 254 in financial contexts, and those that do typically focus on traditional markets such as equities or
 255 macroeconomic data, leaving a gap for cryptocurrency applications. To close this gap, CTBench
 256 evaluates eight state-of-the-art models spanning five families:
 257

- 258 • **GANs: Quant-GAN** (Wiese et al., 2020) and **COSCI-GAN** (Seyfi et al., 2022), applied only in
 259 forecasting tasks since GANs do not natively support reconstruction (Goodfellow et al., 2020).
- 260 • **VAEs: TimeVAE** (Desai et al., 2021) and **KoVAE** (Naiman et al., 2024b), which extend varia-
 261 tional autoencoders for temporal dynamics.
- 262 • **Diffusion Models: Diffusion-TS** (Yuan & Qiao, 2024) and **FIDE** (Galib et al., 2024), leveraging
 263 denoising-based generative processes for time series.
- 264 • **Flow-based Models: Fourier-Flow** (Alaa et al., 2021)), employing invertible transformations for
 265 likelihood-based generation.
- 266 • **Mixed-type Models: LS4** (Zhou et al., 2023), designed to unify strengths across multiple gener-
 267 ative paradigms.

268 These models are selected for their generative fidelity and practical relevance to financial down-
 269 stream tasks. Further details are in Appendix C.5.

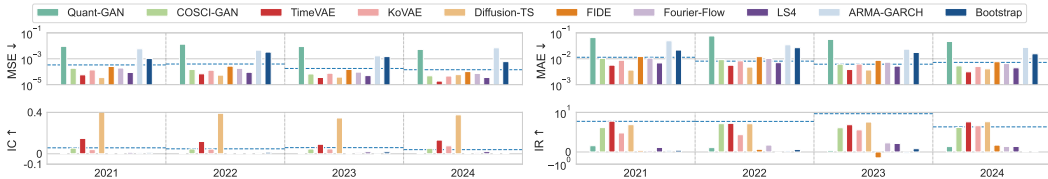


Figure 4: Annual forecasting performance of TSG models on the Predictive Utility task.

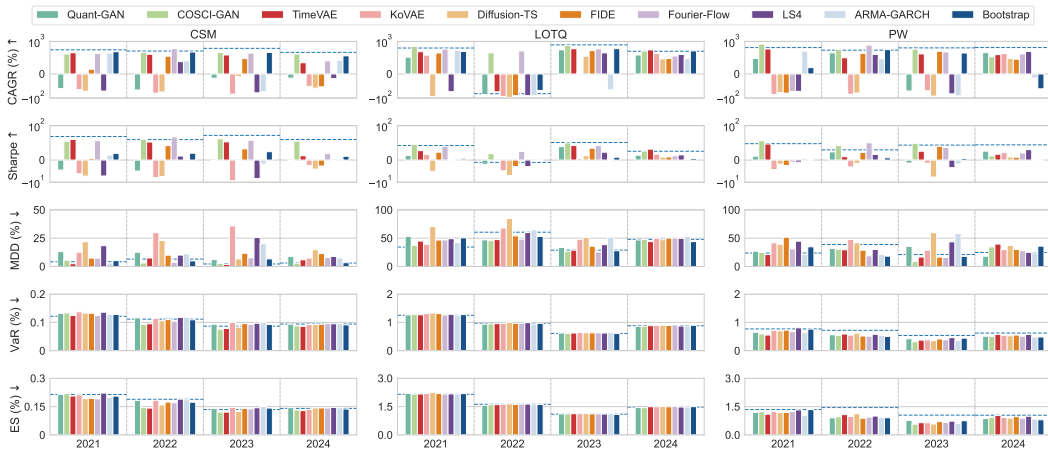


Figure 5: Annual trading performance of TSG models on the Predictive Utility task.

4 EXPERIMENTS

We evaluate CTBench on 452 USDT trading pairs using a walk-forward setup: each cycle trains on 500 days and tests on 30 days (Predictive Utility) or 15 days (Statistical Arbitrage), with retraining before every window. To isolate generator quality, transaction fees are zero by default; for Statistical Arbitrage, we also report results under a 0.03% fee reflecting typical exchange costs Zhang et al. (2023); Winkel & Härdle (2023); Binance Exchange (2025a). We benchmark eight TSG models across five architectural families and include two classical baselines widely used in quantitative finance: **ARMA-GARCH** (Engle, 1982), evaluated on both tasks, and a **Bootstrap** generator (Rubin, 1981), used only for Predictive Utility. All models follow recommended or stable hyperparameters and are scored using CTBench’s full financial metric suite (details in Appendix D).

4.1 PREDICTIVE UTILITY TASK

Figures 4 and 5 report year-wise forecasting and trading performance from 2021 to 2024. The blue dashed line denotes the baseline using real data (without TSG), whose consistently strong returns validate the effectiveness of our feature-extraction pipeline (§3.1).

Annual Predictive Utility Analysis. Across all four market regimes, predictive accuracy and financial profitability often diverge, underscoring the difficulty of converting statistical fidelity into tradable signals. In **2021 (Bull Market)**, Diffusion-TS achieves the best forecasting error yet fails to convert it into returns, while TimeVAE and COSCI-GAN demonstrate strong risk-adjusted performance by balancing denoising and alpha amplification. In **2022 (High Volatility)**, TimeVAE remains resilient, and COSCI-GAN benefits from dispersion, whereas Diffusion-TS struggles with frequent reversals. During **2023 (Consolidation)**, Fourier-Flow outperforms in risk-adjusted metrics due to its frequency-preserving structure, while trend-reliant models degrade. By **2024 (Low-Signal / Mean Reversion)**, Most models face diminishing signal strength; only TimeVAE retains marginal profitability. **Classical baselines ARMA-GARCH and Bootstrap maintain mid-tier performance: solid risk control but limited forecasting capability.** Overall, results show that synthetic data must align with market structure and strategy design, not just minimize reconstruction error.

Ranking Analysis. Radar-plot rankings in Figure 6 reveal three consistent patterns: (1) **Diffusion-TS** achieves the strongest forecasting scores but performs poorly in trading, illustrating a common gap between statistical fidelity and economic usefulness. (2) **TimeVAE** and **COSCI-GAN** show

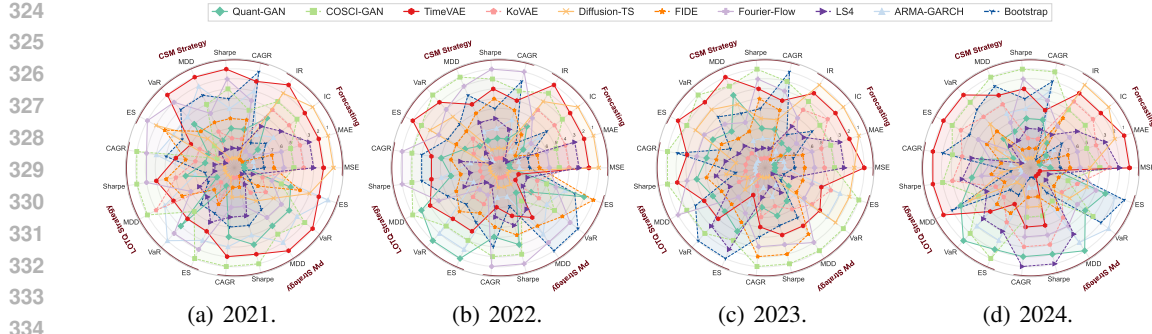


Figure 6: Annual rankings of TSG models on the Predictive Utility task.

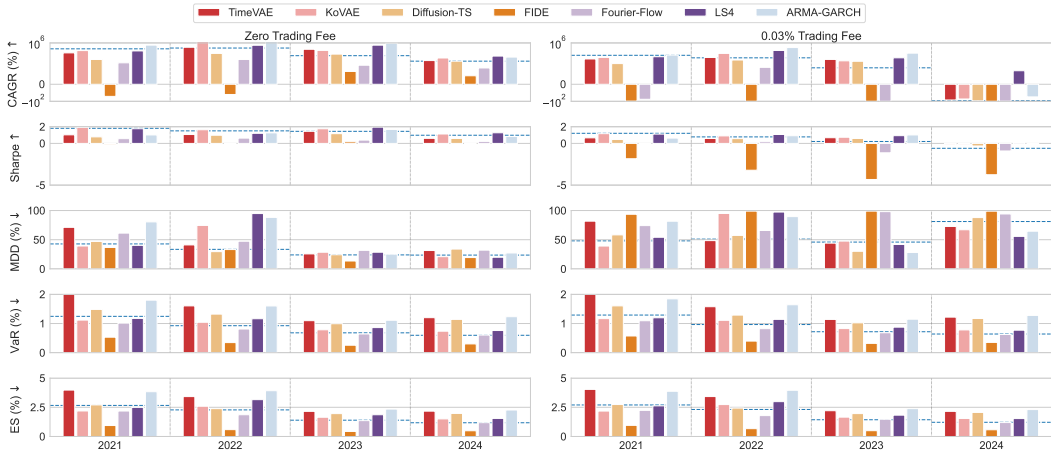


Figure 7: Annual performance of TSG models on the Statistical Arbitrage task.

regime-dependent strengths: TimeVAE excels in stable or mean-reverting markets due to its regularization, while COSCI-GAN benefits from volatile, directional regimes where amplified variance enhances trend signals. (3) **Fourier-Flow** maintains steady mid-to-high rankings across categories, positioning it as a robust, all-weather choice for risk-managed deployment.

These trends reinforce a core insight: *low reconstruction or prediction error does not ensure trading success*. Over-regularization can suppress alpha-bearing variance, while models that preserve structural noise (TimeVAE, COSCI-GAN) produce more actionable signals. Effective model choice must consider market regime and strategy alignment.

Equity Curve Dynamics. Figure 14 presents log-scaled equity curves from 2021–2024 for each TSG model across three trading strategies, highlighting how model inductive biases shape cumulative returns. COSCI-GAN consistently captures directional gains, while TimeVAE and Fourier-Flow provide smoother but moderate returns. Diffusion-based models underperform due to volatility suppression, and LS4 remains conservatively flat. **The ARMA-GARCH baseline similarly yields largely flat. The Bootstrap generator typically sits in the upper middle of the pack, with equity curves that track the top 3-5 models.** Full results and visualizations are in Appendix E.1.

4.2 STATISTICAL ARBITRAGE TASK

Figure 7 reports annualized trading and risk metrics under both zero-fee and realistic-fee conditions. The blue dashed line represents a Principal Component Analysis (PCA) baseline trained on R_{train} , reflecting a standard statistical-arbitrage baseline used as a reference for TSG evaluation.

Annual Performance Analysis. All models exhibit reduced profitability under transaction costs, with the impact tied to turnover. Among TSG models, **KoVAE** excels in volatile regimes with high but mean-reverting swings, whereas **LS4** achieves strong returns with stable drawdowns, particularly in 2023. Even after fees, both maintain leading positions, underscoring the value of regime adaptability and cost-aware design. **TimeVAE** and **Diffusion-TS** form a second tier, trading off

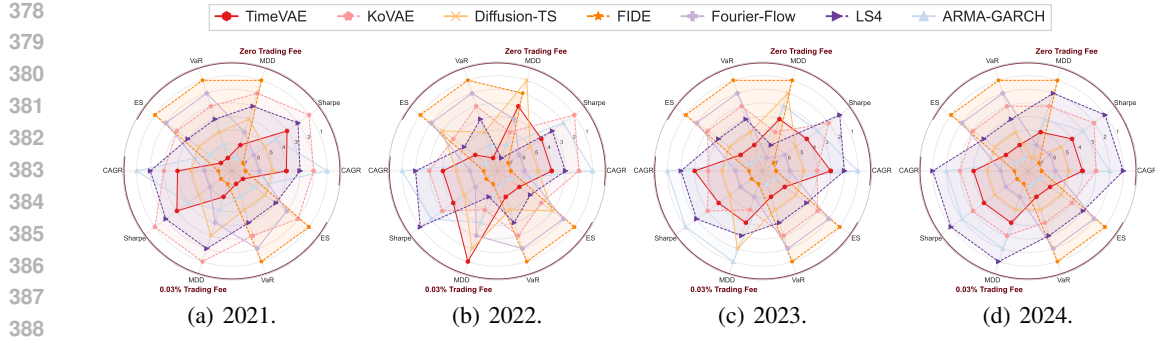


Figure 8: Annual rankings of TSG models on the Statistical Arbitrage task.

peak returns for smoother, fee-resilient SR, though their exposure to tail risk, especially in 2021 and 2024, limits overall efficiency. **FIDE** consistently yields negligible or negative returns but achieves the lowest VaR, ES, and MDD, suggesting over-regularized residuals that suppress tradable variance. **Fourier-Flow** similarly underperforms, failing to capture mean-reverting structure despite effective noise smoothing, highlighting the limitations of exact-likelihood flow models in arbitrage-centric tasks. **ARMA-GARCH** delivers the top CAGR across 2021 to 2023, but consistently exhibits the weakest tail-risk profile, with the worst VaR and ES among all models.

Ranking Analysis. Figure 8 visualizes annual model rankings via radar plots, revealing how TSG models balance return, risk, and stability across regimes. **KoVAE** and **LS4** form polygons that strongly protrude along CAGR and Sharpe but collapse along risk dimensions, indicating high returns paired with elevated drawdown and tail exposure, especially in turbulent years. **FIDE** shows the opposite pattern: tight risk control but consistently weak returns, reflecting a capital-preserving yet alpha-limited design. **TimeVAE** and **Diffusion-TS** produce more rounded, balanced shapes with neither dominant peaks nor severe failures, suggesting steady, regime-agnostic robustness.

Introducing trading fees compresses the rank distances: high-turnover models (e.g., KoVAE) lose several Sharpe positions, whereas smoother, lower-turnover models (e.g., TimeVAE, Diffusion-TS) retain most of their ranking. This highlights an important practical insight: models that generate smoother residual signals naturally incur lower costs and therefore achieve better fee-adjusted performance. Finally, the year-to-year evolution of polygon shapes reveals regime sensitivity: LS4 expands sharply on CAGR in 2023 but suffers high drawdowns in 2022, while KoVAE excels in volatile periods yet underperforms in calmer markets. These dynamics emphasize that model selection must consider both regime characteristics and operational constraints.

Equity Curve Dynamics. Figure 15 illustrates fee-adjusted equity curves starting at \$10,000 with 0.03% trading fees. LS4 and KoVAE deliver sustained growth, while TimeVAE plateaus in later regimes. Diffusion-TS is stable but low-return; FIDE and Fourier-Flow underperform due to overly smoothed residuals. **Remarkably, ARMA-GARCH exhibits moderate gains through early 2023 but experiences substantial growth afterward, ultimately becoming the top-performing model by 2024-2025.** Full results and visualizations are detailed in Appendix E.2.

4.3 EFFICIENCY

We compare training and inference times for all TSG models in Figure 9. VAE-based models are the most efficient: **TimeVAE** trains in under a minute and achieves sub-second inference, making it ideal for real-time applications, low-latency backtesting, and rapid retraining in fast-moving markets. GAN-based models offer moderate efficiency: **COSCI-GAN** maintains balanced runtimes, while **Quant-GAN** is significantly more expensive to train with no corresponding speed advantage at inference. Diffusion-based models are the slowest: **Diffusion-TS** incurs the longest runtimes due to iterative denoising,

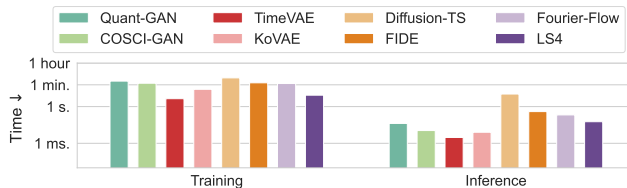


Figure 9: Training and inference time of TSG models.

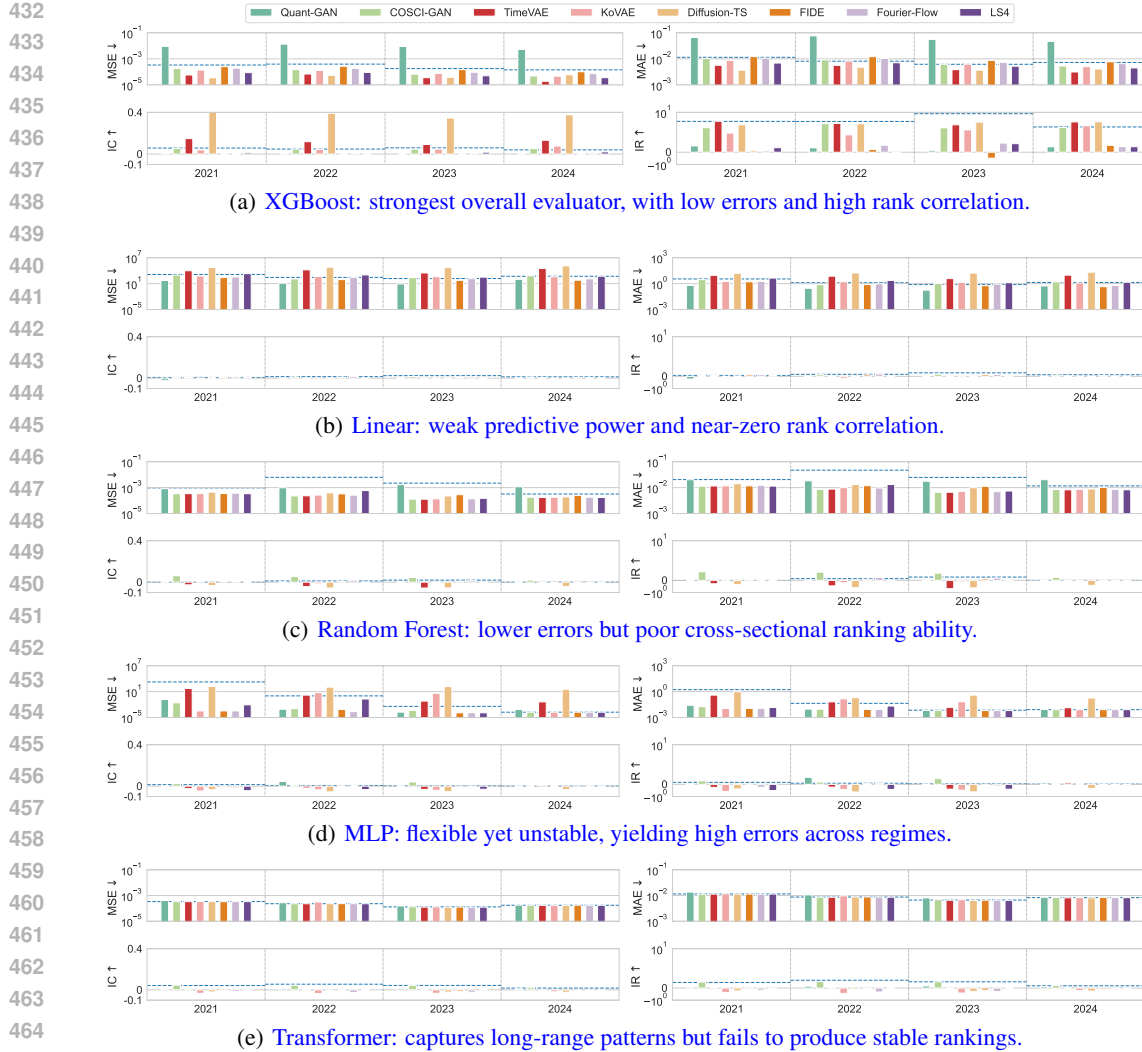


Figure 10: **Ablation** on the choice of forecasting model in the Predictive Utility task. We compare five forecasters: XGBoost, Linear Regression, Random Forest, MLP, and Transformer, to assess whether TSG-model rankings remain stable across evaluators.

and **FIDE** provides only modest improvements. Despite their strong fidelity and risk–return profiles, these models are best suited for offline or compute-rich settings. Flow-based and mixed-type models occupy the middle ground, offering reasonable efficiency and reliable likelihood calibration, though their latency limits real-time use. Overall, **VAE-based models** and **LS4** emerge as the most practical choices for latency-sensitive or resource-constrained deployment, whereas diffusion-based models are better reserved for offline or batch-generation pipelines.

4.4 ABLATION STUDY ON FORECASTING MODELS

A crucial component of the Predictive Utility task is the choice of forecasting model used to assess the quality of synthetic data. In CTBench, we adopt XGBoost (Chen & Guestrin, 2016) as the default forecaster due to its strong empirical performance in quantitative finance and its robustness to heterogeneous, noisy features, properties particularly well aligned with crypto markets (Vancsura et al., 2025; Liu et al., 2021; Yun et al., 2021).

To validate this design choice, we conduct an ablation study comparing five forecasting architectures: XGBoost, Linear Regression (Hilt & Seegrist, 1977), Random Forest (Breiman, 2001), a Multi-Layer Perceptron (MLP) (Hinton, 1990), and a Transformer-based sequence model (Vaswani et al., 2017). Each forecaster is trained on features extracted from identical sets of synthetic data,

486 Table 1: Scenario-based recommendations for selecting TSG models in cryptocurrency markets.
487

488 Scenario	489 Recommendation	490 Rationale
491 Trend-following / Direc- 492 tional Markets	493 COSCI-GAN, KoVAE	494 COSCI-GAN amplifies trend and dispersion; KoVAE offers alpha with higher drawdowns
495 Mean-reverting / Range- 496 bound Regimes	497 TimeVAE, Fourier-Flow, 498 Diffusion-TS	499 TimeVAE / Fourier-Flow provide balance; Diffusion-TS preserves rank order
500 Fee-sensitive / Low- 501 turnover Settings	502 TimeVAE, Diffusion-TS	503 Smooth residuals, stable Sharpe under transaction costs
504 Risk Tolerance / Portfolio 505 Design	506 KoVAE, LS4, TimeVAE, 507 Diffusion-TS, FIDE	508 KoVAE / LS4 maximize returns with risk; TimeVAE / Diffusion-TS balance Sharpe and drawdown; FIDE is defensive
509 Deployment Efficiency	510 TimeVAE, LS4	511 Fast retraining and low-latency inference; diffusion models better suited for offline use

499 ensuring that performance differences arise solely from the forecasting backbone rather than the
500 underlying TSG model. Evaluation follows the same walk-forward protocol as the main benchmark
501 and uses both error-based metrics (MSE, MAE) and rank-based metrics (IC, IR).

502 Figure 10 summarizes the results. **Linear Regression** and **MLP** consistently exhibit high MSE
503 and MAE, indicating poor point-wise prediction accuracy. **Random Forest** and **Transformer** re-
504 duce point-wise errors but fail to preserve cross-sectional ordering, both achieving near-zero IC/IR,
505 suggesting that they primarily fit short-term fluctuations rather than tradable structure. In contrast,
506 **XGBoost** achieves the strongest balance: low prediction error paired with robust rank correlations,
507 making it significantly more sensitive to the differences across TSG models and more aligned with
508 how trading strategies consume forecasts.

509 Overall, the ablation demonstrates that **XGBoost offers the most discriminative and trading-**
510 **relevant evaluation signal**, supporting its use as the default forecaster in CTBench. It consistently
511 reveals meaningful differences between TSG models while avoiding the instability or rank collapse
512 seen in alternative forecasters.

514 4.5 RECOMMENDATIONS

516 Our findings reveal a four-way trade-off among TSG model families: (1) VAE-based models ensure
517 stable reconstruction but might under-react to fast-changing regimes. (2) GAN-based approaches
518 extract trend alpha but suffer from volatility-induced instability. (3) Diffusion models handle regime
519 clustering and fat tails well, but degrade under low signal regimes. (4) Flow-based models prioritize
520 likelihood but offer limited utility, while mixed-type ones are efficient but inconsistent in risk-return.

521 Based on these findings, Table 1 presents actionable guidelines for practitioners. These recom-
522 mendations help align model choice with market conditions, strategic objectives, and operational
523 constraints. Crucially, there is **no one-size-fits-all TSG model** for cryptocurrency markets. In-
524 stead, practitioners should: (1) diagnose the prevailing market regime, alpha source, and system
525 constraints; (2) select a model whose inductive bias strengthens the target structure while preserv-
526 ing tradability; and (3) evaluate performance using task-metric pairs that best reflect production
527 goals. By integrating dual-task design with a comprehensive evaluation suite, CTBench provides
528 the decision surface needed to navigate these choices effectively.

530 5 CONCLUSION AND FUTURE WORK

531 We present CTBench, the first benchmark explicitly designed for time series generation in cryp-
532 toocurrency markets, combining a high-frequency token dataset, a dual-task evaluation framework,
533 and a comprehensive suite of financial metrics to assess both statistical fidelity and practical via-
534 bility. Empirical results reveal key trade-offs across TSG families and highlight strategy-dependent
535 model behaviors, offering actionable insights for real-world deployment.

536 Looking ahead, we plan to enhance CTBench by incorporating more advanced forecasters in the
537 Predictive Utility task and integrating richer residual modeling processes for the Statistical Arbitrage
538 task. Future directions also include expanding to a broader set of tokens, incorporating exogenous
539 signals such as trading volume, and benchmarking more sophisticated generative architectures.

540
541
ETHICS STATEMENT542
543
544
545
The goal of this research is to advance the robustness and relevance of TSG evaluations for financial
applications by incorporating realistic trading tasks, crypto-specific risk metrics, and open-source re-
producibility. We believe this contributes positively to both machine learning research and practical
applications in quantitative finance.546
547
Data Usage. All datasets used in this study are either publicly available or derived from de-identified
and aggregate-level market data, with no inclusion of private or personally identifiable information.548
549
Bias and Fairness. CTBench’s design and metrics aim to capture the unique characteristics of
550
551
552
cryptocurrency markets. However, as with common data-driven benchmarks, models trained on
historical market data might reflect structural biases or artifacts. We encourage further research into
fairness and robustness in financial AI systems, especially in volatile and high-risk domains.553
554
Financial Use Disclaimer. This paper is intended solely for informational and research purposes.
The models, strategies, and market data presented are used to demonstrate our evaluation framework.
555
556
They are not intended as investment research, financial advice, or a recommendation to buy or sell
any financial product. CTBench should not be used to evaluate the merits of any financial transaction
557
or for live trading purposes without further validation.558
559
REPRODUCIBILITY STATEMENT560
561
We are committed to the reproducibility and transparency of CTBench.562
563
Source Code. To facilitate replication and future extensions, we have made our source code publicly
564
565
566
available at the following anonymous repository: <https://anonymous.4open.science/r/CTBench-F5A3/>. It includes all components necessary to reproduce CTBench, such as data
loaders, preprocessing pipelines, task definitions, evaluation measures, and scripts for benchmarking
TSG models.567
568
Datasets. All cryptocurrency datasets used in CTBench are publicly accessible. Detailed descrip-
569
570
tions, token selection criteria, time ranges, and preprocessing steps are provided in Section 3.1 and
Appendix C.1.571
572
Benchmark Design. The benchmark covers eight state-of-the-art TSG models evaluated on Pre-
573
574
575
dictive Utility and Statistical Arbitrage tasks. Implementation details and task formulations are
described in Section 4 and Appendices C–D. The definitions of all evaluation metrics are included
in Section 3.4 and Appendix C.4. Key hyperparameters used for training and evaluation of each
model are summarized in Appendix D to ensure comparability and reproducibility.576
577
Together, these resources provide a complete toolkit for reproducing our results and conducting
future research on TSG in financial domains.578
579
REFERENCES580
581
Ahmed M. Alaa, Alex James Chan, and Mihaela van der Schaar. Generative time-series modeling
582
with fourier flows. In *ICLR*, 2021.583
584
Yihao Ang, Qiang Huang, Yifan Bao, Anthony KH Tung, and Zhiyong Huang. TSGBench: Time
585
Series Generation Benchmark. *Proceedings of the VLDB Endowment*, 17(3):305–318, 2023a.586
587
Yihao Ang, Qiang Huang, Anthony KH Tung, and Zhiyong Huang. A stitch in time saves nine:
588
Enabling early anomaly detection with correlation analysis. In *ICDE*, pp. 1832–1845, 2023b.589
590
Yihao Ang, Yifan Bao, Qiang Huang, Anthony KH Tung, and Zhiyong Huang. TSGAssist: An
591
interactive assistant harnessing LLMs and RAG for time series generation recommendations and
benchmarking. *Proceedings of the VLDB Endowment*, 17(12):4309–4312, 2024.592
593
Yifan Bao, Yihao Ang, Qiang Huang, Anthony KH Tung, and Zhiyong Huang. Towards controllable
time series generation. *arXiv preprint arXiv:2403.03698*, 2024.

- 594 Binance Exchange. Trading fee schedule, 2025a. URL <https://www.binance.com/en/fee/schedule>.
 595
 596
- 597 Binance Exchange. Binance exchange, 2025b. URL <https://binance.com/>.
 598
 599
- 600 Leo Breiman. Random forests. *Machine learning*, 45(1):5–32, 2001.
 601
 602
- 603 Ruichu Cai, Jiawei Chen, Zijian Li, Wei Chen, Keli Zhang, Junjian Ye, Zhuozhang Li, Xiaoyan
 604 Yang, and Zhenjie Zhang. Time series domain adaptation via sparse associative structure align-
 605 ment. In *AAAI*, pp. 6859–6867, 2021.
 606
 607
- 608 Tianqi Chen and Carlos Guestrin. XGBoost: A Scalable Tree Boosting System. In *KDD*, pp. 785–
 609 794, 2016.
 610
 611
- 612 Tianqi Chen, Yulia Rubanova, Jesse Bettencourt, and David Duvenaud. Neural Ordinary Differential
 613 Equations. In *NeurIPS*, pp. 6572–6583, 2018.
 614
 615
- 616 Zhicheng Chen, FENG SHIBO, Zhong Zhang, Xi Xiao, Xingyu Gao, and Peilin Zhao. SDFormer:
 617 similarity-driven discrete transformer for time series generation. In *NeurIPS*, pp. 132179–132207,
 618 2024.
 619
 620
- 621 Andrea Coletta, Sriram Gopalakrishnan, Daniel Borrajo, and Svitlana Vyetrenko. On the con-
 622 strained time-series generation problem. In *NeurIPS*, pp. 61048–61059, 2023.
 623
 624
- 625 Ruizhi Deng, Bo Chang, Marcus A. Brubaker, Greg Mori, and Andreas M. Lehrmann. Modeling
 626 continuous stochastic processes with dynamic normalizing flows. In *NeurIPS*, pp. 7805–7815,
 627 2020.
 628
 629
- 630 Abhyuday Desai, Cynthia Freeman, Zuhui Wang, and Ian Beaver. Timevae: A variational auto-
 631 encoder for multivariate time series generation. *arXiv preprint arXiv:2111.08095*, 2021.
 632
 633
- 634 Chris Donahue, Julian J. McAuley, and Miller S. Puckette. Adversarial audio synthesis. In *ICLR*,
 635 2019.
 636
 637
- 638 Robert F Engle. Autoregressive conditional heteroscedasticity with estimates of the variance of
 639 united kingdom inflation. *Econometrica: Journal of the Econometric Society*, pp. 987–1007,
 640 1982.
 641
 642
- 643 Cristóbal Esteban, Stephanie L Hyland, and Gunnar Rätsch. Real-valued (medical) time series
 644 generation with recurrent conditional gans. *arXiv preprint arXiv:1706.02633*, 2017.
 645
 646
- 647 Asadullah Hill Galib, Pang-Ning Tan, and Lifeng Luo. FIDE: Frequency-Inflated Conditional Diffu-
 648 sion Model for Extreme-Aware Time Series Generation. In *NeurIPS*, pp. 114434–114457, 2024.
 649
 650
- 651 Ian Goodfellow, Jean Pouget-Abadie, Mehdi Mirza, Bing Xu, David Warde-Farley, Sherjil Ozair,
 652 Aaron Courville, and Yoshua Bengio. Generative Adversarial Networks. *Communications of the
 653 ACM*, 63(11):139–144, 2020.
 654
 655
- 656 Donald E Hilt and Donald W Seegrist. *Ridge, a computer program for calculating ridge regression
 657 estimates*, volume 236. Department of Agriculture, Forest Service, Northeastern Forest Experi-
 658 ment, 1977.
 659
 660
- 661 Geoffrey E Hinton. Connectionist learning procedures. In *Machine learning*, pp. 555–610. 1990.
 662
 663
- 664 Yang Hu, Xiao Wang, Lirong Wu, Huatian Zhang, Stan Z Li, Sheng Wang, and Tianlong Chen.
 665 FM-TS: Flow Matching for Time Series Generation. *arXiv preprint arXiv:2411.07506*, 2024.
 666
 667
- 668 Yifan Hu, Yuante Li, Peiyuan Liu, Yuxia Zhu, Naiqi Li, Tao Dai, Shu-tao Xia, Dawei Cheng, and
 669 Changjun Jiang. FinTSB: a comprehensive and practical benchmark for financial time series
 670 forecasting. *arXiv preprint arXiv:2502.18834*, 2025.
 671
 672
- 673 Daniel Jarrett, Ioana Bica, and Mihaela van der Schaar. Time-series generation by contrastive imi-
 674 tation. In *NeurIPS*, pp. 28968–28982, 2021.
 675
 676

- 648 Paul Jeha, Michael Bohlke-Schneider, Pedro Mercado, Shubham Kapoor, Rajbir Singh Nirwan,
 649 Valentin Flunkert, Jan Gasthaus, and Tim Januschowski. Psa-gan: Progressive self attention gans
 650 for synthetic time series. In *ICLR*, 2021.
- 651
- 652 Jinsung Jeon, Jeonghak Kim, Haryong Song, Seunghyeon Cho, and Noseong Park. GT-GAN: gen-
 653 eral purpose time series synthesis with generative adversarial networks. In *NeurIPS*, pp. 36999–
 654 37010, 2022.
- 655 James Jordon, Jinsung Yoon, and Mihaela Van Der Schaar. PATE-GAN: Generating synthetic data
 656 with differential privacy guarantees. In *ICLR*, 2018.
- 657
- 658 Zura Kakushadze. 101 formulaic alphas. *Wilmott*, 2016(84):72–81, 2016.
- 659
- 660 Patrick Kidger, James Foster, Xuechen Li, and Terry J Lyons. Neural SDEs as Infinite-Dimensional
 661 GANs. In *ICML*, pp. 5453–5463, 2021.
- 662
- 663 Daesoo Lee, Sara Malacarne, and Erlend Aune. Vector quantized time series generation with a
 664 bidirectional prior model. In *AISTATS*, pp. 7665–7693, 2023.
- 665
- 666 Hongming Li, Shujian Yu, and Jose Principe. Causal recurrent variational autoencoder for medical
 667 time series generation. In *AAAI*, pp. 8562–8570, 2023.
- 668
- 669 Xiaomin Li, Vangelis Metsis, Huangyingrui Wang, and Anne Hee Hiong Ngu. TTS-GAN: A
 670 transformer-based time-series generative adversarial network. In *AIME*, pp. 133–143, 2022a.
- 671
- 672 Yang Li, Han Meng, Zhenyu Bi, Ingolv T. Urnes, and Haipeng Chen. Population aware diffusion
 673 for time series generation. In *AAAI*, pp. 18520–18529, 2025.
- 674
- 675 Yueling Li, Zhengzhang Chen, Daochen Zha, Mengnan Du, Jingchao Ni, Denghui Zhang, Haifeng
 676 Chen, and Xia Hu. Towards learning disentangled representations for time series. In *KDD*, pp.
 677 3270–3278, 2022b.
- 678
- 679 Haksoo Lim, Minjung Kim, Sewon Park, and Noseong Park. Regular Time-series Generation using
 680 SGM. *arXiv preprint arXiv:2301.08518*, 2023.
- 681
- 682 Zinan Lin, Alankar Jain, Chen Wang, Giulia Fanti, and Vyas Sekar. Using gans for sharing net-
 683 worked time series data: Challenges, initial promise, and open questions. In *Proceedings of the
 684 ACM Internet Measurement Conference*, pp. 464–483, 2020.
- 685
- 686 Guang Liu, Yuzhao Mao, Qi Sun, Hailong Huang, Weiguo Gao, Xuan Li, Jianping Shen, Ruifan Li,
 687 and Xiaojie Wang. Multi-scale two-way deep neural network for stock trend prediction. In *IJCAI*,
 688 pp. 4555–4561, 2021.
- 689
- 690 Yuansan Liu, Sudanthi Wijewickrema, Ang Li, and James Bailey. Time-Transformer AAE: Con-
 691 nnecting Temporal Convolutional Networks and Transformer for Time Series Generation, 2023.
 692 URL https://openreview.net/forum?id=fI3y_Dajlca.
- 693
- 694 Olof Mogren. C-rnn-gan: A continuous recurrent neural network with adversarial training. In
 695 *Constructive Machine Learning Workshop (CML) at NIPS 2016*, pp. 1, 2016.
- 696
- 697 Ilan Naiman, Nimrod Berman, Itai Pemper, Idan Arbib, Gal Fadlon, and Omri Azencot. Utilizing
 698 image transforms and diffusion models for generative modeling of short and long time series. In
 699 *NeurIPS*, pp. 121699–121730, 2024a.
- 700
- 701 Ilan Naiman, N. Benjamin Erichson, Pu Ren, Michael W. Mahoney, and Omri Azencot. Generative
 702 modeling of regular and irregular time series data via koopman VAEs. In *ICLR*, 2024b.
- 703
- 704 Hao Ni, Lukasz Szpruch, Magnus Wiese, Shujian Liao, and Baoren Xiao. Conditional Sig-
 705 Wasserstein GANs for Time Series Generation. *arXiv preprint arXiv:2006.05421*, 2020.
- 706
- 707 Hao Ni, Lukasz Szpruch, Marc Sabate-Vidales, Baoren Xiao, Magnus Wiese, and Shujian Liao. Sig-
 708 Wasserstein GANs for time series generation. In *Proceedings of the Second ACM International
 709 Conference on AI in Finance*, pp. 1–8, 2021.

- 702 Alexander Nikitin, Letizia Iannucci, and Samuel Kaski. TSGM: A Flexible Framework for Genera-
 703 tive Modeling of Synthetic Time Series. *arXiv preprint arXiv:2305.11567*, 2023.
 704
- 705 Hengzhi Pei, Kan Ren, Yuqing Yang, Chang Liu, Tao Qin, and Dongsheng Li. Towards generating
 706 real-world time series data. In *ICDM*, pp. 469–478, 2021.
 707
- 708 Jian Qian, Bingyu Xie, Biao Wan, Minhao Li, Miao Sun, and Patrick Yin Chiang. TimeLDM: Latent
 709 Diffusion Model for Unconditional Time Series Generation. *arXiv preprint arXiv:2407.04211*,
 710 2024.
- 711 Xiangfei Qiu, Jilin Hu, Lekui Zhou, Xingjian Wu, Junyang Du, Buang Zhang, Chenjuan Guo,
 712 Aoying Zhou, Christian S Jensen, Zhenli Sheng, et al. Tfb: Towards comprehensive and fair
 713 benchmarking of time series forecasting methods. *Proceedings of the VLDB Endowment*, 17(9):
 714 2363–2377, 2024.
- 715 Giorgia Ramponi, Pavlos Protopapas, Marco Brambilla, and Ryan Janssen. T-CGAN: conditional
 716 generative adversarial network for data augmentation in noisy time series with irregular sampling.
 717 *arXiv preprint arXiv:1811.08295*, 2018.
- 718 Carl Remlinger, Joseph Mikael, and Romuald Elie. Conditional loss and deep euler scheme for time
 719 series generation. In *AAAI*, pp. 8098–8105, 2022.
 720
- 721 Reuters. Crypto sector breaches \$4 trillion in market value during pivotal week. *Reuters*, 2025.
- 722 Yulia Rubanova, Ricky T. Q. Chen, and David K Duvenaud. Latent ordinary differential equations
 723 for irregularly-sampled time series. In *NeurIPS*, pp. 5320–5330, 2019.
 724
- 725 Donald B Rubin. The bayesian bootstrap. *The Annals of Statistics*, pp. 130–134, 1981.
- 726 Ali Seyfi, Jean-François Rajotte, and Raymond T. Ng. Generating multivariate time series with
 727 common source coordinated GAN (COSCI-GAN). In *NeurIPS*, pp. 32777–32788, 2022.
 728
- 729 Kaleb E Smith and Anthony O Smith. Conditional GAN for Timeseries Generation. *arXiv preprint*
 730 *arXiv:2006.16477*, 2020.
- 731 Padmanaba Srinivasan and William J Knottenbelt. Time-series transformer generative adversarial
 732 networks. *arXiv preprint arXiv:2205.11164*, 2022.
 733
- 734 Shuo Sun, Rundong Wang, and Bo An. Reinforcement learning for quantitative trading. *ACM*
 735 *Transactions on Intelligent Systems and Technology*, 14(3):1–29, 2023.
- 736 Muhang Tian, Bernie Chen, Allan Guo, Shiyi Jiang, and Anru R Zhang. Reliable generation of
 737 privacy-preserving synthetic electronic health record time series via diffusion models. *Journal of*
 738 *the American Medical Informatics Association*, 31(11):2529–2539, 2024.
 739
- 740 Chih-Fong Tsai and Yu-Chieh Hsiao. Combining multiple feature selection methods for stock pre-
 741 diction: Union, intersection, and multi-intersection approaches. *Decision Support Systems*, 50(1):
 742 258–269, 2010.
- 743 George E Uhlenbeck and Leonard S Ornstein. On the theory of the brownian motion. *Physical*
 744 *Review*, 36(5):823, 1930.
- 745 László Vancsura, Tibor Tatay, and Tibor Bareith. Navigating ai-driven financial forecasting: A
 746 systematic review of current status and critical research gaps. *Forecasting*, 7(3):36, 2025.
 747
- 748 Ashish Vaswani, Noam Shazeer, Niki Parmar, Jakob Uszkoreit, Llion Jones, Aidan N Gomez,
 749 Łukasz Kaiser, and Illia Polosukhin. Attention is all you need. In *Proceedings of the 31st Inter-
 750 national Conference on Neural Information Processing Systems (NIPS)*, pp. 6000–6010, 2017.
- 751 Chengyu Wang, Kui Wu, Tongqing Zhou, Guang Yu, and Zhiping Cai. Tsagen: synthetic time series
 752 generation for kpi anomaly detection. *IEEE Transactions on Network and Service Management*,
 753 19(1):130–145, 2021.
 754
- 755 Lei Wang, Liang Zeng, and Jian Li. AEC-GAN: adversarial error correction gans for auto-regressive
 long time-series generation. In *AAAI*, pp. 10140–10148, 2023.

- 756 Yanlong Wang, Jian Xu, Tiantian Gao, Hongkang Zhang, Shao-Lun Huang, Danny Dongning Sun,
 757 and Xiao-Ping Zhang. FinTSBridge: A New Evaluation Suite for Real-world Financial Prediction
 758 with Advanced Time Series Models. *arXiv preprint arXiv:2503.06928*, 2025.
- 759
- 760 Magnus Wiese, Robert Knobloch, Ralf Korn, and Peter Kretschmer. Quant GANs: deep generation
 761 of financial time series. *Quantitative Finance*, 20(9):1419–1440, 2020.
- 762
- 763 Julian Winkel and Wolfgang Karl Härdle. Pricing kernels and risk premia implied in bitcoin options.
 764 *Risks*, 11(5):85, 2023.
- 765
- 766 Tianlin Xu, Li Kevin Wenliang, Michael Munn, and Beatrice Acciaio. COT-GAN: generating se-
 767 quential data via causal optimal transport. In *NeurIPS*, pp. 8798–8809, 2020.
- 768
- 769 Jinsung Yoon, Daniel Jarrett, and Mihaela van der Schaar. Time-series generative adversarial net-
 770 works. In *NeurIPS*, pp. 5509–5519, 2019.
- 771
- 772 Xinyu Yuan and Yan Qiao. Diffusion-TS: Interpretable Diffusion for General Time Series Genera-
 773 tion. In *ICLR*, 2024.
- 774
- 775 Kyung Keun Yun, Sang Won Yoon, and Daehan Won. Prediction of stock price direction using a
 776 hybrid ga-xgboost algorithm with a three-stage feature engineering process. *Expert Systems with
 777 Applications*, 186:115716, 2021.
- 778
- 779 Chuheng Zhang, Yuanqi Li, Xi Chen, Yifei Jin, Pingzhong Tang, and Jian Li. Doubleensemble:
 780 A new ensemble method based on sample reweighting and feature selection for financial data
 781 analysis. In *ICDM*, pp. 781–790, 2020.
- 782
- 783 Chuheng Zhang, Yitong Duan, Xiaoyu Chen, Jianyu Chen, Jian Li, and Li Zhao. Towards general-
 784 izable reinforcement learning for trade execution. In *IJCAI*, pp. 4975–4983, 2023.
- 785
- 786 Linqi Zhou, Michael Poli, Winnie Xu, Stefano Massaroli, and Stefano Ermon. Deep latent state
 787 space models for time-series generation. In *ICML*, pp. 42625–42643, 2023.
- 788
- 789 Zhoufan Zhu and Ke Zhu. AlphaQCM: Alpha discovery in finance with distributional reinforce-
 790 ment learning. In *ICML*, 2025. URL <https://openreview.net/forum?id=3sXMH1hBSs>.
- 791

A NOTATIONS

792 Table 2 summarizes the symbols and definitions used throughout the paper for quick reference.

793

794 Table 2: List of frequently used notations.

795

796 Symbol	797 Description
798 $\mathbf{R} \in \mathbb{R}^{n \times l}$	799 Log-return matrix with n assets and l hourly observations
800 $\mathbf{r}_t = [r_{i,t}] \in \mathbb{R}^n$	801 Log-return vector of time t of all n assets
802 w, s, k, τ	803 Training window size, test step, # of splits, split offset
804 $\mathbf{R}_{\text{train}}, \mathbf{R}_{\text{test}}$	805 Training data of returns, test data of returns
806 \mathbf{g}	807 Time series generation (TSG) model
808 $\mathbf{R}_{\text{gen}}, \hat{\mathbf{R}}_{\text{train}}, \hat{\mathbf{R}}_{\text{test}}$	809 Generated time series, reconstruction of train and test sets
810 $\boldsymbol{\eta}_t = [\eta_{i,t}] \in \mathbb{R}^n$	811 Portfolio weight vector at hour t
812 V_0, V_t , and ΔV_t	813 Initial capital, portfolio equity, and profit-and-loss at hour t
814 O, H, L, C	815 Open, High, Low, and Close (OHLC) prices
816 $\mathbf{D} = [\mathbf{x}_{i,t}]$	817 Multi-asset OHLC data array
818 $\Phi = \{\phi_j\}_{j=1}^d$	819 A feature set Φ with d feature mapping function ϕ_j

810
811

B SCOPE ILLUSTRATION

812 To ensure clarity and fairness in benchmarking, CTBench explicitly defines its scope across datasets,
813 strategies, evaluation measures, and model families. This scoped design avoids confounding factors,
814 emphasizes crypto-specific characteristics, and provides a standardized basis for comparing diverse
815 TSG methods. The followings detail these design choices.816 **Scope of Datasets.** CTBench is restricted to cryptocurrency markets due to their unique properties,
817 such as 24/7 trading, high volatility, and fragmented liquidity. In selecting the concrete dataset,
818 we focus on Binance USDT spot pairs Binance Exchange (2025b) because Binance is consistently
819 ranked as the largest centralized exchange by global spot volume and provides broad, liquid coverage
820 of actively traded assets. Its freely accessible, high-quality historical data ensures that CTBench
821 remains fully reproducible without requiring proprietary data contracts.822 Moreover, we use only raw time series inputs (i.e., returns), excluding side-channel information
823 (e.g., order books, blockchain logs, or news). This isolates core generative capabilities without
824 reliance on auxiliary signals. We employ only well-established financial features (e.g., Alpha101
825 (Kakushadze, 2016)) to ensure compatibility with real-world quantitative trading while minimizing
826 noise from complex feature engineering.827 **Scope of Trading Strategies.** To capture diverse trading behaviors, we benchmark TSG models
828 across three canonical strategies, ranging from rank-based to magnitude-sensitive and from direc-
829 tional to market-neutral setups. This ensures a holistic evaluation of whether synthetic data general-
830 izes across real-world trading paradigms or merely overfits to specific signal patterns.831 **Scope of Evaluation Measures.** Our benchmark incorporates a curated set of evaluation measures
832 widely recognized in financial TSG research (Ang et al., 2023a; Wiese et al., 2020), ensuring a
833 holistic assessment of statistical fidelity and financial utility. We have excluded metrics with limited
834 practical relevance or interpretability to maintain a focused and meaningful evaluation framework
835 for the crypto domain.836 **Scope of TSG Models.** We select TSG models capable of handling multivariate inputs typical in
837 crypto markets, encompassing both general-purpose and finance-specific architectures. Our selec-
838 tion spans five model families: GAN, VAE, diffusion, flow, and mixed-type, favoring architectures
839 with general applicability over domain-specific requirements. All models are trained under a unified
840 protocol without excessive hyperparameter tuning to ensure fair benchmarking and reflect practical
841 deployment constraints.842
843

C BENCHMARK DETAILS

844

C.1 CRYPTO-CENTRIC DATASETS

845 **Data Descriptive Statistics.** Understanding the statistical profile of crypto returns is essential for
846 designing effective TSG benchmarks. We analyze the distribution of log-returns to identify devi-
847 ations from normality, such as skewness and kurtosis, stylized facts well documented in financial
848 time series. Cryptocurrencies, in particular, often exhibit **fat-tailed distributions**, indicating ele-
849 vated probability of extreme price movements.850 Figure 11 presents histograms of the mean hourly log-return and mean hourly volatility (standard
851 deviation of log-returns) across all 452 cryptocurrencies. The mean hourly returns are centered
852 around zero but show a slight right skew, suggesting modestly positive drift in most assets. In
853 contrast, the mean hourly volatility exhibits a long right tail, indicating that while many assets trade
854 with low volatility, a notable subset experiences highly volatile price swings.855 To visualize market dynamics over time, we categorize cryptocurrencies into large-, mid-, and small-
856 cap groups and plot representative closing prices annually from 2020 to 2024 in Figure 12. These
857 trajectories highlight significant market regimes, including the bull runs of 2020–2021, sharp cor-
858 rections in 2022, and subsequent periods of recovery or consolidation. Notably, mid- and small-cap
859 assets often display greater volatility and sharper price swings than their large-cap counterparts.860 Given that cryptocurrency markets operate 24/7, intraday patterns provide valuable insights into mar-
861 ket microstructure. Figure 13 depicts the mean hourly log-return and volatility by time of day. We

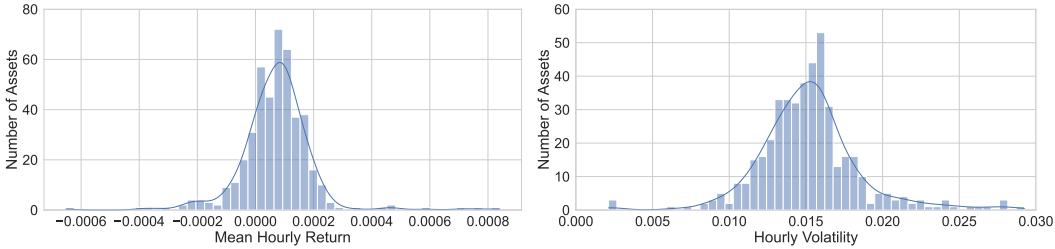


Figure 11: Histograms of the mean hourly log-return (%) (left) and mean hourly volatility (%) (right).

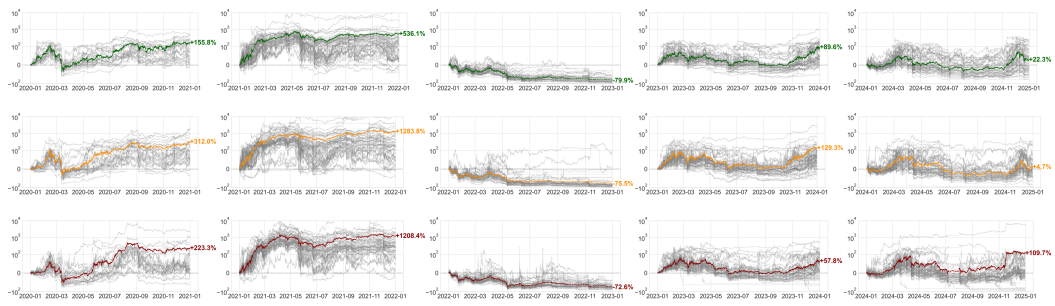


Figure 12: Line plots of closing returns for representative cryptocurrencies, with large-cap examples (top row), mid-cap examples (middle row), and small-cap examples (bottom row), displayed annually from 2020 to 2024.

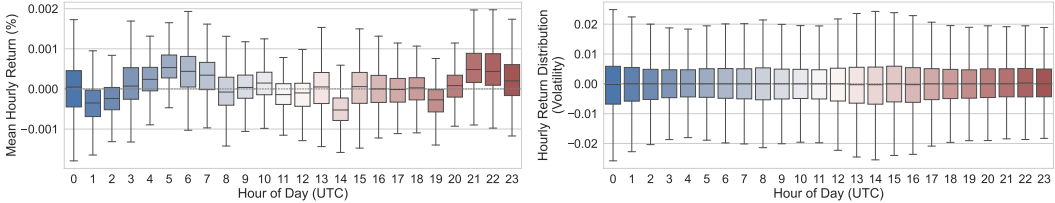


Figure 13: The mean hourly log-return (%) (left) and mean hourly volatility (%) (right) by hour of day (UTC).

observe return peaks around early morning (5–7 AM) and late evening (9–11 PM), reflecting heightened trading during transitions between major global financial centers. Volatility peaks notably around midnight and during overlapping trading hours between US and Europe (12–5 PM), suggesting periods of intensified market activity driven by global participation and algorithmic strategies.

Discussions. Our analysis reveals several critical insights shaping the design of CTBench:

- **Complex Market Dynamics:** Crypto markets exhibit high-frequency, high-dimensional behaviors with distinct volatility profiles, intraday cycles, and regime shifts. These factors necessitate benchmarks tailored for crypto time series.
- **Benchmark Task Design:** Given the data’s complexity, evaluation tasks must probe whether synthetic data preserves predictive structures critical for practical applications such as forecasting and statistical arbitrage.
- **TSG Model Requirements:** Capturing the intricate temporal and cross-sectional dependencies of crypto markets demands advanced TSG architectures capable of modeling both short-term fluctuations and long-term trends.
- **Evaluation Metrics:** Assessing TSG performance in crypto markets requires multifaceted metrics that go beyond statistical fidelity to capture financial viability and risk sensitivity.

Collectively, these insights underscore the need for crypto-specific benchmarks like CTBench to advance the evaluation and development of TSG models for this rapidly evolving domain.

918 C.2 DUAL-TASK EVALUATION
919920 C.2.1 PREDICTIVE UTILITY TASK
921

922 **Training Phase.** Let $\mathbf{R}_{\text{train}}^{(\tau)} = [\mathbf{r}_{\tau-w+1}, \dots, \mathbf{r}_\tau] \in \mathbb{R}^{n \times w}$ denote the real log-return matrix for a
923 split offset τ with length $w = 500 \times 24$ hours. A TSG model \mathbf{g} is trained on $\mathbf{R}_{\text{train}}^{(\tau)}$ to capture
924 both temporal dependencies and cross-sectional relationships. From this trained model, we sample
925 synthetic returns:

$$926 \quad \mathbf{R}_{\text{gen}} = \mathbf{g}(\mathbf{z}), \mathbf{z} \sim \mathcal{N}(\mathbf{0}, \mathbf{I}).$$

927 Next, features are extracted from \mathbf{R}_{gen} via the pipeline: $\Phi(\mathbf{R}_{\text{gen}}) \in \mathbb{R}^{n \times s \times d}$. A forecasting model
928 $\mathbf{f} : \mathbb{R}^d \rightarrow \mathbb{R}$ then predicts the next-hour return:

$$929 \quad \hat{r}_{i,t+1} = \mathbf{f}(\Phi(\mathbf{R}_{\text{gen}})[i, t, :]).$$

931 We use XGBoost (Chen & Guestrin, 2016) as the forecasting model, chosen for its balance of robust-
932 ness, interpretability, and minimal hyperparameter tuning (Vancsura et al., 2025; Liu et al., 2021;
933 Yun et al., 2021), ensuring that benchmark results primarily reflect the quality of the generated data
934 rather than model capacity.

935 **Trading Phase.** The trained forecaster is then applied to a test period of length $s = 30 \times 24$
936 hours. For each hour t and asset i , we predict $\hat{r}_{i,t+1} = \mathbf{f}(\Phi(\mathbf{R}_{\text{test}})[i, t, :])$, rank the vector
937 $\hat{\mathbf{r}}_{t+1} = [\hat{r}_{i,t+1}]_{i=1}^n$, and construct a dollar-neutral portfolio by **longing** the top half of assets (highest
938 $\hat{r}_{i,t+1}$) and **shorting** the bottom half (lowest $\hat{r}_{i,t+1}$). This portfolio is rebalanced hourly over the test
939 window, maintaining balanced long and short exposures.

940 **Discussions.** This task reveals how well synthetic data generalizes to real markets, operationalizing
941 the notion of functional realism. If \mathbf{R}_{gen} preserves the predictive structures of $\mathbf{R}_{\text{train}}^{(\tau)}$, the realized
942 P&L ΔV_t will score highly across CTBench’s evaluation suite. Thus, synthetic data are valued not
943 merely for statistical closeness to historical distributions but for the economic utility they unlock.
944 Importantly, every component in Figure 3(a) is modular: researchers can substitute alternative TSG
945 models, forecasters (e.g., Transformers), or feature sets, while retaining a unified scoring framework.

947 C.2.2 STATISTICAL ARBITRAGE TASK
948

949 **Training Phase.** The Statistical Arbitrage task typically hinges on pairs or baskets of assets whose
950 spreads revert toward a long-term mean. In this task, residuals between real $\mathbf{R}_{\text{train}}$ and reconstructed
951 returns $\hat{\mathbf{R}}_{\text{train}}$ are assumed to follow mean-reverting dynamics. For asset i and time t , we define
952 training residual:

$$953 \quad \rho_{i,t} = r_{i,t} - \hat{r}_{i,t},$$

954 where $r_{i,t} \in \mathbf{R}_{\text{train}}$ and $\hat{r}_{i,t} \in \hat{\mathbf{R}}_{\text{train}}$. For each asset i , these residuals are then fitted to an Ornstein-
955 Uhlenbeck (OU) process (Uhlenbeck & Ornstein, 1930):

$$956 \quad d\rho_{i,t} = \theta_i(\mu_i - \rho_{i,t})dt + \sigma_i dW_t,$$

958 where $\theta_i > 0$ (mean reversion speed), μ_i (long-run mean), and σ_i (volatility) are estimated per asset,
959 and dW_t is a standard Wiener increment.

960 **Trading Phase.** On test data \mathbf{R}_{test} , the model reconstructs returns $\hat{\mathbf{R}}_{\text{test}}$, producing test residuals for
961 $r_{i,t} \in \mathbf{R}_{\text{test}}$ and $\hat{r}_{i,t} \in \hat{\mathbf{R}}_{\text{test}}$:

$$962 \quad \epsilon_{i,t} = r_{i,t} - \hat{r}_{i,t}.$$

963 Each residual $\epsilon_{i,t}$ is converted to an s -score:

$$965 \quad s_{i,t} = \frac{\epsilon_{i,t} - \mu_i}{\sigma_i / \sqrt{2\theta_i}},$$

967 quantifying the deviation from equilibrium. Trading signals are then derived via:

- 969 **Thresholding:** Open or maintain a short position if $s_{i,t} > +\gamma$, a long if $s_{i,t} < -\gamma$, otherwise
970 stay flat, with $\gamma = 2$.
- 971 **Weight Normalization:** Raw signals $\eta_{i,t} = \text{sgn}(-s_{i,t}) \cdot |s_{i,t}|$ are normalized to $\tilde{\eta}_{i,t} =$
972 $\eta_{i,t} / (\sum_j |\eta_{j,t}|)$.

- 972 • **Execution:** Portfolios are rebalanced hourly based on $\hat{\eta}_{i,t}$.

973
 974 **Discussions.** The Statistical Arbitrage task evaluates whether reconstructed time series reveal stable,
 975 mean-reverting residuals suitable for statistical arbitrage, complementing the generation-focused
 976 task by addressing market-neutral alpha extraction. These tasks ensure TSG models are tested not
 977 only for statistical fidelity but also for practical effectiveness in real-world crypto trading.

978 **C.3 TRADING STRATEGIES**

980 Beyond the datasets and dual-task evaluation, trading strategies play a central role in assessing
 981 whether synthetic time series capture signals that are economically meaningful. Since no single
 982 strategy can fully characterize market behavior, CTBench incorporates multiple paradigms that re-
 983 flect how practitioners deploy forecasts in real trading:

- 984 • **S1: Cross-Sectional Momentum (CSM)** takes long positions in the top decile and short posi-
 985 tions in the bottom decile of assets ranked by predicted one-hour returns. This probes a model’s
 986 ability to capture ranking-based alpha signals.
- 987 • **S2: Long-Only Top-Quantile (LOTQ)** equally weights and goes long in the top 20% of assets
 988 based on predicted returns, with all other weights set to zero. This isolates pure directional signals
 989 without short exposure.
- 990 • **S3: Proportional-Weighting (PW)** allocates weights proportionally to predicted returns: $\eta_{i,t} =$
 991 $\hat{r}_{i,t}/(\sum_{j=1}^n \hat{r}_{j,t})$, emphasizing the magnitude of forecasted signals rather than merely their ranks.

992 Each strategy exploits different statistical regularities, including level effects, cross-sectional disper-
 993 sion, and serial correlations, ensuring that no single modeling flaw remains undetected. They span
 994 the primary mandates seen on crypto desks: beta-neutral long–short equity, directional trend cap-
 995 ture, and volatility harvesting. Finally, the CTBench pipeline is fully **plug-and-play**. Traders can
 996 drop in any proprietary strategies without altering the benchmark code, fostering fair comparison
 997 across future studies.

998 **C.4 FINANCIAL METRIC SUITE**

1000 Evaluating TSG models in crypto requires more than statistical similarity, it demands metrics that
 1001 connect directly to financial relevance and practical usability. To this end, CTBench employs a
 1002 structured suite of measures that balance fidelity, predictive utility, trading performance, and risk
 1003 management, while also accounting for computational efficiency.

1004 **Error-based Evaluation.** Given the actual return $r_{i,t}$ and prediction $\hat{r}_{i,t}$ for asset i and time t :

- 1005 • **E1: Mean Squared Error (MSE)** is defined as:

$$1006 \text{MSE} = \frac{1}{k \cdot s \cdot n} \sum_{\tau \in \mathcal{O}} \sum_{t=1}^s \sum_{i=1}^n (r_{i,t+\tau} - \hat{r}_{i,t+\tau})^2.$$

- 1007 • **E2: Mean Absolute Error (MAE)** is defined as

$$1008 \text{MAE} = \frac{1}{k \cdot s \cdot n} \sum_{\tau \in \mathcal{O}} \sum_{t=1}^s \sum_{i=1}^n |r_{i,t+\tau} - \hat{r}_{i,t+\tau}|.$$

1009 Low values in both metrics reflect strong signal fidelity, while differences help distinguish outliers
 1010 from widespread minor errors.

1011 **Rank-based Evaluation.** Given realized returns r_t and predictions \hat{r}_t for all assets at time t :

- 1012 • **E3: Information Coefficient (IC)** is defined as the average Spearman correlation between pre-
 1013 dicted and actual rankings, where $\text{IC}_{\tau,t} = \text{SpearmanCorr}(r_{t+\tau}, \hat{r}_{t+\tau})$. It is computed as:

$$1014 \text{IC} = \frac{1}{k \cdot s} \sum_{\tau \in \mathcal{O}} \sum_{t=1}^s \text{IC}_{\tau,t}.$$

- 1015 • **E4: Information Ratio (IR)** measures the stability of IC:

$$1016 \text{IR} = \frac{\text{Mean}(\text{IC}_{\tau,t})}{\text{Std}(\text{IC}_{\tau,t})}.$$

1026 A consistently positive IC shows the generator preserves rankings essential for long-short strategies,
 1027 despite absolute errors.
 1028

1029 **Trading Performance.** To assess economic utility, we evaluate both profitability and risk-adjusted
 1030 returns using the hourly profit-and-loss ΔV_t and the simple return of equity $\Delta V_t/V_{t-1}$ at time t :

- 1031 • **E5: Compound Annual Growth Rate (CAGR)** captures the annualized return based on equity
 1032 growth, where V_0 and V_s are the initial and final equity. It is calculated as:

$$1033 \quad 1034 \quad \text{CAGR} = \left(\frac{V_s}{V_0} \right)^{8760/s} - 1. \\ 1035$$

- 1036 • **E6: Sharpe Ratio (SR)** is defined as:

$$1037 \quad 1038 \quad \text{SR} = \frac{\mathbb{E}[\Delta V_t/V_{t-1}]}{\text{Std}(\Delta V_t/V_{t-1})} \cdot \sqrt{8760}. \\ 1039$$

1040 These metrics capture both returns and the risk profile of synthetic-data-driven strategies.

1041 **Risk Assessment Metrics.** Given profit-and-loss series ΔV_t and simple return of equity $\Delta V_t/V_{t-1}$:

- 1042 • **E7: Maximum Drawdown (MDD)** is defined as:

$$1043 \quad 1044 \quad \text{MDD} = \max_{u \leq t} \left(\frac{V_u - V_t}{V_u} \right). \\ 1045$$

- 1046 • **E8: Value at Risk (VaR)** at 95% confidence is defined as:

$$1047 \quad 1048 \quad \text{VaR}_{0.95} = -\text{Percentile}_{5\%}(\Delta V_t/V_{t-1}).$$

- 1049 • **E9: Expected Shortfall (ES)** at 95% confidence is defined as:

$$1050 \quad 1051 \quad \text{ES}_{0.95} = -\mathbb{E}[(\Delta V_t/V_{t-1}) \mid (\Delta V_t/V_{t-1}) \leq -\text{VaR}_{0.95}].$$

1052 VaR captures potential worst-day losses, while ES reveals mean loss beyond that threshold, offering
 1053 a fuller picture of tail risk.

1054 **Efficiency.** CTBench evaluates efficiency along two dimensions: training and inference time, to
 1055 capture both scalability during model development and responsiveness in real-time use.

- 1056 • **E10: Training Time** is the wall-clock time at which a TSG model is trained.

- 1057 • **E11: Inference Time** is the mean wall-clock time to generate or reconstruct one batch of data (n
 1058 assets \times s time steps).

1061 C.5 TSG MODEL ZOO

1062 **GAN-based Methods.** These methods (Seyfi et al., 2022; Wiese et al., 2020; Pei et al., 2021; Wang
 1063 et al., 2023) leverage adversarial training to generate realistic series. They incorporate recurrent
 1064 neural architectures and specialized attention mechanisms tailored to temporal dependencies.

- 1065 • **M1: Quant-GAN (Wiese et al., 2020)** approximates a trading utility function, optimizing the
 1066 generator for downstream profitability.
 1067 • **M2: COSCI-GAN (Seyfi et al., 2022)** integrates causal self-attention and statistical conditioning
 1068 to consider temporal order and cross-asset correlations.

1069 **VAE-based Methods.** These Methods use variational inference to capture both local and global
 1070 temporal patterns (Desai et al., 2021; Lee et al., 2023; Li et al., 2023). They have shown strong
 1071 performance in general TSG tasks (Ang et al., 2023a; Bao et al., 2024).

- 1072 • **M3: TimeVAE (Desai et al., 2021)** is a sequence-aware VAE with temporal convolutions, de-
 1073 signed to capture both local and long-range dependencies in multivariate time series.
 1074 • **M4: KoVAE (Naiman et al., 2024b)** enhances TimeVAE by incorporating Koopman operator-
 1075 based latent dynamics for smoother and more interpretable generation.

1076 **Diffusion-based Methods.** Diffusion models (Yuan & Qiao, 2024; Galib et al., 2024; Chen et al.,
 1077 2024; Li et al., 2025; Naiman et al., 2024a) progressively convert noise into structured data via
 1078 iterative denoising, proving highly effective in modeling complex market dynamics.

Table 3: Summary of popular TSG methods with their backbone models and financial datasets used.

Year	Method	Backbone	Financial Datasets Used
2016	C-RNN-GAN (Mogren, 2016)	GAN	/
2017	RCGAN (Esteban et al., 2017)	GAN	/
2018	T-CGAN (Rapponi et al., 2018)	GAN	/
2019	TimeGAN (Yoon et al., 2019)	GAN	Stocks
2019	WaveGAN (Donahue et al., 2019)	GAN	/
2020	COT-GAN (Xu et al., 2020)	GAN	/
2020	DoppelGANger (Lin et al., 2020)	GAN	/
2020	Quant-GAN (Wiese et al., 2020)	GAN	SPX
2020	SigCWGAN (Ni et al., 2020)	GAN	SPX & DJI
2020	TSGAN (Smith & Smith, 2020)	GAN	/
2021	RTSGAN (Pei et al., 2021)	GAN	Stocks
2021	Sig-WGAN (Ni et al., 2021)	GAN	SPX & DJI
2021	TimeGCI (Jarrett et al., 2021)	GAN	/
2022	CEGEN (Remlinger et al., 2022)	GAN	Stocks & Electric Price
2022	COSCI-GAN (Seyfi et al., 2022)	GAN	/
2022	PSA-GAN (Jeha et al., 2021)	GAN	/
2022	TsT-GAN (Srinivasan & Knottenbelt, 2022)	GAN	Stocks
2022	TTS-GAN (Li et al., 2022a)	GAN	/
2023	AEC-GAN (Wang et al., 2023)	GAN	/
2023	TT-AAE (Liu et al., 2023)	GAN	Stocks
2021	TimeVAE (Desai et al., 2021)	VAE	Stocks
2023	CRVAE (Li et al., 2023)	VAE	/
2023	TimeVQVAE (Lee et al., 2023)	VAE	/
2024	KoVAE (Naiman et al., 2024b)	VAE	Stocks
2023	DiffTime (Coletta et al., 2023)	Diffusion	Stocks
2023	TSGM (Lim et al., 2023)	Diffusion	Stocks
2024	Diffusion-TS (Yuan & Qiao, 2024)	Diffusion	Stocks
2024	FIDE (Galib et al., 2024)	Diffusion	Stocks
2024	ImagenTime (Naiman et al., 2024a)	Diffusion	Stocks
2024	SDformer (Chen et al., 2024)	Diffusion	Stocks
2025	PaD-TS (Li et al., 2025)	Diffusion	Stocks
2020	CTFP (Deng et al., 2020)	Flow	/
2021	Fourier-Flow (Alaa et al., 2021)	Flow	Stocks
2024	FlowTS (Hu et al., 2024)	Flow	Stocks
2018	Neural ODE (Chen et al., 2018)	ODE + RNN	/
2019	ODE-RNN (Rubanova et al., 2019)	ODE + RNN	/
2021	Neural SDE (Kidger et al., 2021)	ODE + GAN	Stocks
2022	GT-GAN (Jeon et al., 2022)	ODE + GAN	Stocks
2023	LS4 (Zhou et al., 2023)	ODE + VAE	/
2024	TimeLDM (Qian et al., 2024)	Diffusion + VAE	Stocks

- **M5: Diffusion-TS (Yuan & Qiao, 2024)** is a score-based diffusion model that refines Gaussian noise into realistic trajectories, achieving state-of-the-art sample fidelity on financial data.
- **M6: FIDE (Galib et al., 2024)** introduces factorized conditional diffusion with attention-driven score networks, enabling conditional generation based on market regimes or liquidity factors.

Flow-based Methods. These methods (Alaa et al., 2021; Hu et al., 2024) employ invertible transformations to model data distributions, ensuring exact likelihood estimation and efficient sampling.

- 1134 • **M7: Fourier-Flow (Alaa et al., 2021)** uses frequency-domain coupling layers for invertible
 1135 transformations, allowing fast sampling and exact likelihood computation while preserving pe-
 1136 riodic structures.

1137 **Mixed-based Methods.** Hybrid models (Zhou et al., 2023; Rubanova et al., 2019; Jeon et al., 2022)
 1138 typically combine multiple modeling paradigms (e.g., ODEs and VAEs) to capture nuanced temporal
 1139 dynamics and stochastic characteristics.

- 1140 • **M8: LS4 (Zhou et al., 2023)** fuses deep state-space modeling with stochastic latent variables via
 1141 variational inference, providing flexible and interpretable modeling of complex crypto dynamics.

1144 D EXPERIMENTAL SETUP

1145 **Datasets.** We employ the datasets (Binance Exchange, 2025b) described in §3.1 for the experiments.
 1146 To simulate real-world deployment, we adopt a walk-forward rolling-window validation scheme,
 1147 using 500 days of hourly data for training, and 30 or 15 days for testing on the Predictive Utility and
 1148 Statistical Arbitrage tasks, respectively. After each cycle, the window advances by the test period
 1149 length, with models retrained. This process spans from January 2020 to December 2024, covering
 1150 diverse market regimes.

1151 **Benchmark Configurations.** To isolate core TSG model performance, we assume zero trading
 1152 fees by default in both Predictive Utility and Statistical Arbitrage tasks, enabling fair comparison
 1153 of signal quality without interference from platform-specific costs. For the Statistical Arbitrage
 1154 task, we also apply a 0.03% trading fee, reflecting the fee level that a typical liquidity provider
 1155 can achieve on major centralized exchanges (Zhang et al., 2023; Winkel & Härdle, 2023; Binance
 1156 Exchange, 2025a), providing a more grounded evaluation of net profitability.

1157 **Trading Strategies.** For the Predictive Utility task, we employ three representative trading strate-
 1158 gies in §3.3 to evaluate synthetic data across varied portfolio constructions. In contrast, the Statis-
 1159 tical Arbitrage task employs the mean-reversion strategy to isolate the model’s ability to preserve
 1160 exploitable residual structures.

1161 **TSG Methods.** We evaluate eight representative TSG models across five major families in §3.5.
 1162 Hyperparameter settings follow published recommendations or are tuned for stable training.

- 1163 • **GAN-based:** Quant-GAN adopts $\text{latent_dim} = 8$, $\text{hidden_dim} = 80$, gradient penalty $\lambda_{\text{gp}} = 10.0$,
 1164 and critic steps $n_{\text{critic}} = 5$; COSCI-GAN uses $\text{latent_dim} = 32$, $\gamma = 5$, and $n_{\text{groups}} = 4$ with
 1165 MLP-based central discriminators, as per (Seyfi et al., 2022).
- 1166 • **VAE-based:** TimeVAE uses $\text{latent_dim} = 8$ with stacked hidden layers of 50, 100, and 200 units;
 1167 KoVAE follows (Naiman et al., 2024b), setting $W_{\text{KL}} = 0.009$ and $W_{\text{PRED}} = 0.03$ for KL and
 1168 auxiliary loss terms.
- 1169 • **Diffusion-based:** Diffusion-TS uses 1000 timesteps, 3 encoder layers, 6 decoder layers, and
 1170 $d_{\text{model}} = 64$; FIDE applies 1000 steps, $\text{hidden_dim} = 64$, 8 layers, and $\sigma = 0.05$.
- 1171 • **Flow-based:** Fourier-Flow incorporates DFT-based coupling layers with $\text{hidden_size} = 128$ and 3
 1172 flow layers.
- 1173 • **Mixed-type:** LS4 employs $\text{hidden_dim} = 6$, $\text{latent_dim} = 8$, and a batch size of 512.

1174 **Financial Baseline Models.** We added two baselines commonly used in quantitative finance:

- 1175 • **ARMA-GARCH** (Engle, 1982): We fit multivariate VAR-DCC-GARCH models, which are
 1176 multivariate extensions of univariate ARMA-GARCH models, to jointly capture the conditional
 1177 mean, volatility, and dynamic correlation structure of returns. Specifically, we use a VAR(1)
 1178 specification for the conditional mean (corresponding to an ARMA(1,0) structure in each marginal
 1179 series), univariate GARCH(1,1) processes for the conditional variances, and a DCC(1,1) structure
 1180 for the time-varying conditional correlations.
- 1181 • **Bootstrap** (Rubin, 1981): We implement a bootstrap-style generator that resamples returns to
 1182 preserve marginal distributions and local dependence structures without explicit parametric dy-
 1183 namics.

1184 These models are evaluated under the same Predictive Utility task as the learning-based TSG models.
 1185 In addition, for the Statistical Arbitrage task, we use the ARMA-GARCH model’s filtered (fitted)
 1186 conditional mean process as reconstructions as in Section 3.2.

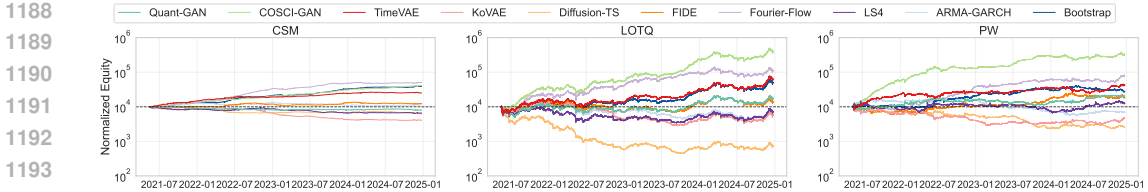


Figure 14: Simulated growth curves of \$10,000 over four years under three trading strategies.

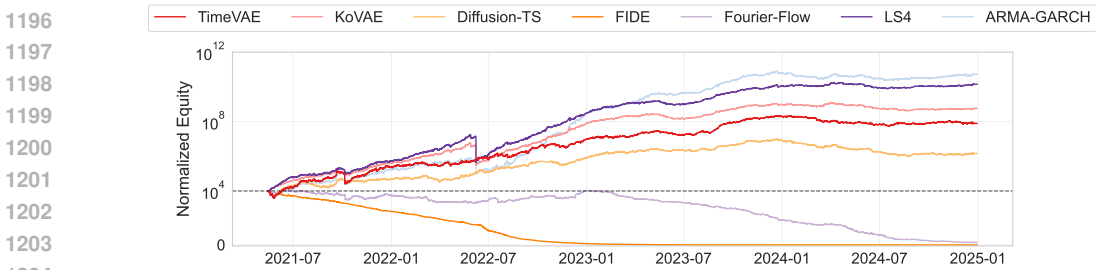


Figure 15: Simulated growth curves of \$10,000 for the Statistical Arbitrage task (with 0.03% fee).

Evaluation Metrics. We adopt the thirteen metrics detailed in §3.4, thereby scoring each model on forecasting accuracy, rank correlation, trading profitability, tail risk, and computational efficiency.

Experiments Environments. All experiments are conducted on a machine equipped with an Intel® Xeon® Platinum 8480C @3.80GHz, 64 GB RAM, and an NVIDIA H100 GPU.

E ADDITIONAL RESULTS ON EQUITY CURVE DYNAMICS

E.1 PREDICTIVE UTILITY TASK

Figure 14 presents log-scaled equity curves (initialized at \$10,000) for each TSG model under three trading strategies from 2021 to 2024, highlighting cumulative returns and how inductive biases interact with shifting market regimes.

Under **CSM**, COSCI-GAN and TimeVAE deliver steady gains by effectively preserving rank order and alpha signals, though both limit upside potential by dampening extreme winners. In contrast, Diffusion-TS and FIDE exhibit persistent declines, as their denoising processes suppress volatility and weaken long-short execution.

Under **LOTQ**, COSCI-GAN clearly outperforms, likely benefiting from adversarially enhanced right-tail signals that capture strong directional momentum. TimeVAE and Fourier-Flow sustain modest but stable growth, whereas Diffusion-TS falters by missing rare yet critical upward spikes.

Finally, under **PW**, which emphasizes consistent pairwise rankings, COSCI-GAN again dominates. TimeVAE and Fourier-Flow show smooth compounding, reflecting robust generalization from well-regularized latent spaces. By contrast, LS4 remains largely flat across all strategies, suggesting its conservative design behaves more like a low-beta portfolio than an alpha-generating model.

E.2 STATISTICAL ARBITRAGE TASK

Figure 15 illustrates the equity curves under the Statistical Arbitrage task, starting from \$10,000 and incorporating 0.03% trading fees.

At the top end, LS4 compounds almost monotonically, underscoring its strong fee resilience, with two staircase-like surges in mid-2022 and early 2023. This pattern suggests that its latent-switching mechanism is particularly effective at capturing regime shifts rather than merely reacting to incremental mean-reversion. KoVAE follows with a similarly convex trajectory, initially smooth with shallow drawdowns through 2023, though its growth fades amid the turbulence of 2024. TimeVAE maintains steady gains through 2022, plateaus in mid-2023, and drifts sideways or slightly downward in 2024, reflecting its dependence on residual signals that weaken as cross-sectional dispersion compresses.

1242 Among mid-tier performers, Diffusion-TS delivers a notably stable curve with minimal drawdowns,
1243 though its terminal return is the lowest among viable models, consistent with its characterization as
1244 a fee-resilient, risk-balanced generator.

1245 At the lower end, FIDE collapses early, suggesting that its residuals may be over-regularized to the
1246 point of eliminating tradable structure. Meanwhile, Fourier-Flow experiences a slow but persistent
1247 bleed after mid-2022, likely driven by over-smoothed residual patterns that generate a sustained
1248 negative carry.

1250 **F THE USE OF LARGE LANGUAGE MODELS (LLMs)**

1251 LLMs are used mainly as auxiliary tools to aid and polish the writing of the paper.

1252
1253
1254
1255
1256
1257
1258
1259
1260
1261
1262
1263
1264
1265
1266
1267
1268
1269
1270
1271
1272
1273
1274
1275
1276
1277
1278
1279
1280
1281
1282
1283
1284
1285
1286
1287
1288
1289
1290
1291
1292
1293
1294
1295